

FAST TRACK COMMUNICATION

Uncovering multiple orbitals influence in high harmonic generation from aligned N₂

Anh-Thu Le¹, R R Lucchese² and C D Lin¹¹ Department of Physics, Cardwell Hall, Kansas State University, Manhattan, KS 66506, USA² Department of Chemistry, Texas A&M University, College Station, TX 77843-3255, USAE-mail: atle@phys.ksu.edu

Received 18 September 2009, in final form 3 October 2009

Published 27 October 2009

Online at stacks.iop.org/JPhysB/42/211001**Abstract**

Recent measurements on high-order harmonic generation (HHG) from N₂ aligned perpendicular to the driving laser polarization (B K McFarland *et al* 2008 *Science* **322** 1232) have shown a maximum at the rotational half-revival. This has been interpreted as the signature of the HHG contribution from the molecular orbital just below the highest occupied molecular orbital (HOMO). By using the recently developed quantitative rescattering theory combined with accurate photoionization transition dipoles, we show that the maximum at the rotational half-revival is indeed associated with the HOMO-1 contribution. Our results also show that the HOMO-1 contribution becomes increasingly more important near the HHG cutoff and therefore depends on the laser intensity.

(Some figures in this article are in colour only in the electronic version)

High-order harmonic generation (HHG) has been extensively investigated both experimentally and theoretically over the last two decades [1]. Until very recently, the HHG has been understood as being due to tunnelling ionization of an electron from the highest occupied molecular orbital (HOMO) and recombining back to the HOMO. The contribution from lower molecular orbitals is routinely neglected. That is not surprising since tunnelling is a highly nonlinear process, and therefore highly selective to the HOMO due to energy considerations. In general, the neglect of the contribution from lower molecular orbitals is not justified for systems where the HOMO and HOMO-1 are nearly degenerate, in other words, when the energy gap between the HOMO and lower molecular orbitals is much smaller than the ionization potential from the HOMO. Furthermore, for some molecular alignments, tunnelling ionization from the HOMO is suppressed due to symmetry of the wavefunction [2]. Clearly, in that case, the neglect of lower molecular orbitals is questionable. These two favourable conditions for observing a HOMO-1 contribution are present in N₂, where the $1\pi_u$ HOMO-1 has a binding energy of 16.93 eV, quite close to the binding energy of the $3\sigma_g$ HOMO (15.58 eV).

Early theoretical calculations based on the strong-field approximation (SFA) model [3, 4] have shown that harmonic yields from aligned N₂ are maximum if the molecules are aligned along the laser polarization direction. These results are in good agreements with the pump-probe delay time experimental data [5, 6] as well as the recent more direct measurements [7]. On the other hand, the contribution from the HOMO-1 is expected to peak near 90°. Although the two molecular orbitals contribute to different alignment regions in the total harmonic yields, it is still a very challenging task to disentangle the HOMO-1 since its contribution is expected to be relatively weak. This is in strong contrast to the traditional single-photon photoionization where electrons are generally ionized from many MOs with comparable strengths (see, for example, [8]).

In a recent experiment, McFarland *et al* [9] reported that they have successfully observed the contribution from the HOMO-1 in aligned N₂. That has been achieved within the pump-probe scheme with perpendicular pump-probe polarizations. For low harmonic orders below H23, the harmonic signals behave similarly to *inverted* $\langle \cos^2 \theta \rangle$, i.e. inverse of the degree of molecular alignment or $1 - \langle \cos^2 \theta \rangle$. For higher harmonics, McFarland *et al* observed a maximum

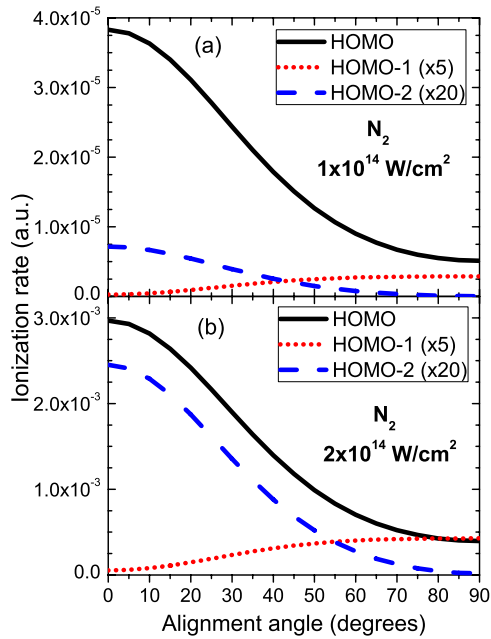


Figure 1. Ionization rates from HOMO, HOMO-1 and HOMO-2 at laser intensities of 1×10^{14} (a) and 2×10^{14} W cm^{-2} (b). The data from HOMO-1 and HOMO-2 have been multiplied by a factor of 5 and 20, respectively. Calculations are carried out within the MO-ADK theory.

at the rotational half-revival, where *inverted* ($\cos^2 \theta$) is minimum. Furthermore, the maximum at the half-revival is found to be quite pronounced in the HHG cutoff region, the location of which depends on the intensity of the driving laser.

The goal of this paper is to show theoretically that the main features observed by McFarland *et al* [9] are indeed the signature of the HOMO-1 contribution. To support our claim, we have carried out calculations by using the recently developed quantitative rescattering theory (QRS) [10]. The photoionization transition dipole and its phase are obtained from state-of-the-art molecular photoionization calculations [11, 12]. The QRS theory is based on the rescattering picture and it has been shown to give accurate results comparable with that from the time-dependent Schrödinger equation (TDSE) for rare-gas atoms [13, 14] and the molecular ion H_2^+ [15]. The QRS has also been shown to be able to reproduce most of the available experiments on aligned molecules CO_2 , O_2 and N_2 [10, 16]. Other applications of the QRS include calculations of high-energy above-threshold ionization momentum and energy spectra (see, for example, [17] and references therein) and nonsequential double ionization [18]. Analytical derivations for the QRS have been reported quite recently in [19–21]. In this paper, we extend the QRS theory [10] to the multi-channel case, where the contribution from each channel to the total induced dipole is added coherently. We assume that the ion cores are frozen during the time interval between ionization and photo-recombination.

First, we note that the HOMO ($3\sigma_g$), HOMO-1 ($1\pi_u$) and HOMO-2 ($2\sigma_u$) have binding energies of 15.58, 16.93 and 18.73 eV, respectively. In order to have an idea about the magnitude of the relative contributions from the HOMO,

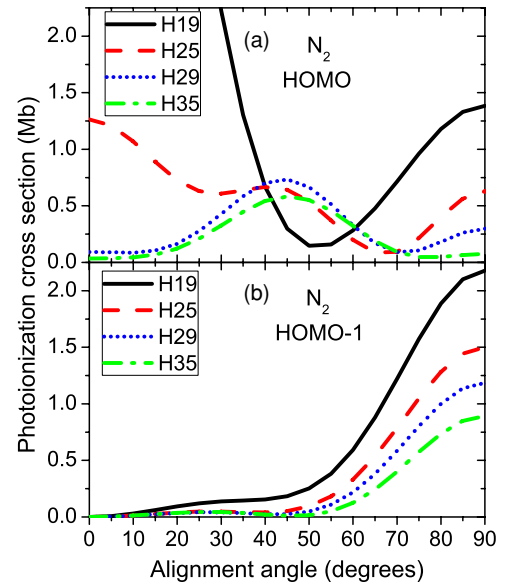


Figure 2. Differential photoionization cross sections versus alignment angle from HOMO (a) and HOMO-1 (b) for some selected energies (expressed in units of harmonic orders for an 800 nm laser).

HOMO-1 and HOMO-2 in the returning electron wave packet, we compare the ionization rates from these molecular orbitals. These comparisons are shown in figure 1 for two different laser intensities of 1×10^{14} and 2×10^{14} W cm^{-2} . The calculations were performed within the molecular tunnelling (MO-ADK) theory [2]. The MO-ADK C_l coefficients were calculated from asymptotic wavefunctions of each orbital, which in turn were obtained from the *GAUSSIAN* code [22]. Clearly the ionization rates depend strongly on the alignment and the alignment-dependent rates are different for different symmetries of the orbitals. This fact has been known before for HOMOs both theoretically [23, 24] and experimentally [25, 26]. For the HOMO-1 ($1\pi_u$), the ionization rate peaks near 90° . Within this range of laser intensity, the rate from the HOMO-1 is a factor of 5 smaller than that of the HOMO, even at 90° . For the HOMO-2 ($2\sigma_u$), the ionization rate peaks near 0° , similar to that of the HOMO. However, its magnitude is significantly smaller than that of the HOMO (approximately by a factor of 20 for this range of laser intensity). We note that the relative contributions from the lower orbitals become increasingly more important as the laser intensity increases. We also carried out calculations using the SFA and found similar angular dependence for ionization rates from these three MOs. The relative strengths are also in good agreement with the MO-ADK, although the rate for the HOMO-2 from the SFA seems to be enhanced by a factor of 5 (i.e. still about a factor of 10 weaker than the HOMO). We note that our results do not agree with the recent results from the time-dependent density-functional theory calculations [27], which show a peak in the ionization rate from the HOMO-1 at an intermediate angle.

The above analysis shows that the contribution to the returning wave packet from the HOMO-1 is about a factor of 5 smaller than that of the HOMO even near its peak at 90° . Can the HOMO-1 contribution to the harmonic generation be

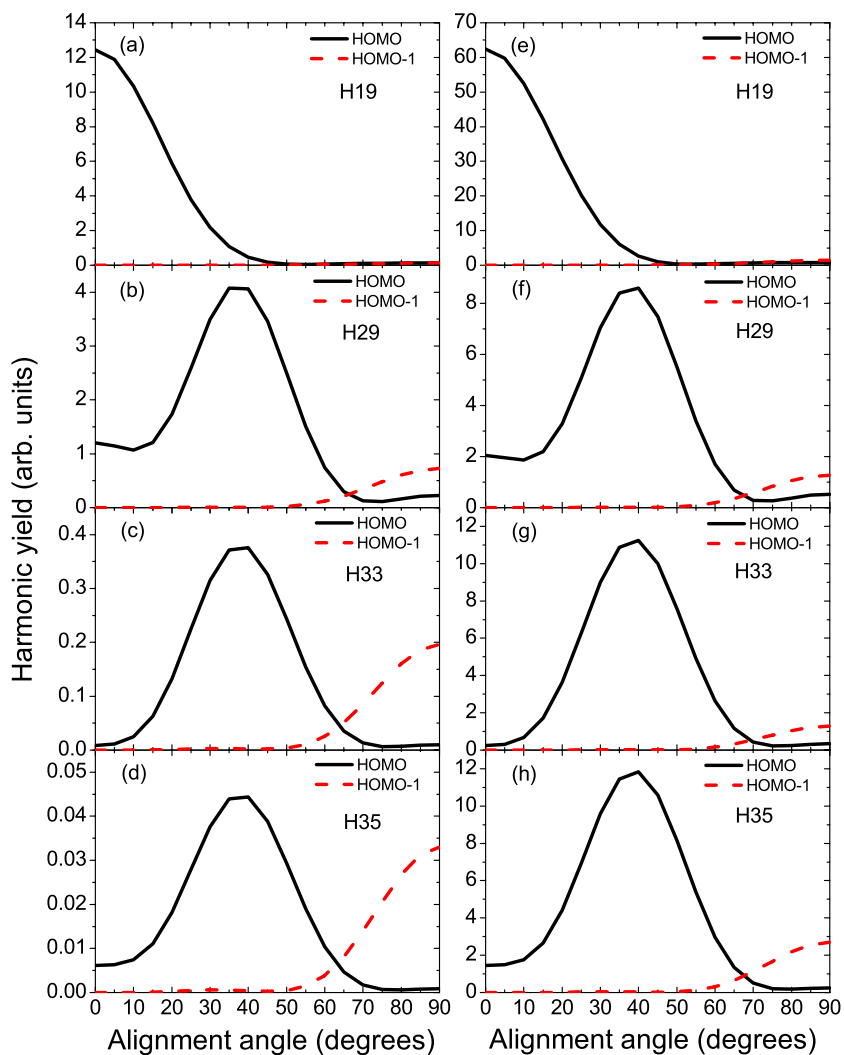


Figure 3. Contributions to HHG yields from HOMO and HOMO-1 for some selected harmonics with the laser intensity of $1.5 \times 10^{14} \text{ W cm}^{-2}$ (left column) and $2 \times 10^{14} \text{ W cm}^{-2}$ (right column). Molecular axis is assumed to be fixed (no averaging over alignment distribution was carried out).

comparable with that of the HOMO? To answer this question, we show in figure 2(a) the comparison of the differential photoionization cross sections from the HOMO and HOMO-1. (In this paper, we limit ourselves to the harmonics with polarization parallel to that of the driving laser. Therefore, the relevant differential cross sections are for the electron emitted along the laser polarization direction [10].) For convenience, we express photon energy in units of the photon energy of the 800 nm laser (1.55 eV). First, we note that the cross sections from the HOMO vary strongly from one energy to the next. Nevertheless, one general feature that can be seen is that the cross sections at large angles near 90° are quite small, say about 0.25 Mb for H29, and decrease quickly with energy. On the other hand, the photoionization cross sections from the HOMO-1 all have a dominant peak at 90° , which reaches 1.25 Mb for H29. Recall that according to the QRS theory, HHG yield is proportional to a product of the returning wave packet and the differential photoionization cross section. The results shown in figures 1 and 2 therefore indicate that the HOMO and HOMO-1 contributions could be comparable near 90° .

Having established qualitatively that the contribution from the HOMO-1 cannot be neglected for large angles, we now analyse the HHG yields from the actual QRS calculations. In figures 3(a)–(d) (left column), we show the HHG yields from the HOMO and HOMO-1 for H19, H29, H33 and H35. The 800 nm laser pulse is of 30 fs duration (FWHM) and intensity of $1.5 \times 10^{14} \text{ W cm}^{-2}$. Clearly, the HOMO contribution dominates for alignment angles smaller than 45° for all the harmonics. For large angles the HOMO-1 becomes comparable with the HOMO already near H25 and dominates for the higher harmonics, especially beyond the cutoff at H29. Similar pattern repeats at a higher laser intensity of $2 \times 10^{14} \text{ W cm}^{-2}$, shown in figures 3(e)–(h) (right column). However, the HOMO-1 is only comparable with the HOMO at large angles for H29 and it starts to dominate only at higher harmonics. The enhanced contribution from the HOMO-1 near the cutoff can be understood as the consequence of the delay in the harmonic cutoff for the HOMO-1, since the ionization potential from the HOMO-1 is about 1.5 eV greater than that from the HOMO. As the cutoff moves to near H35 for the laser intensity of $2 \times 10^{14} \text{ W cm}^{-2}$, the HOMO-1

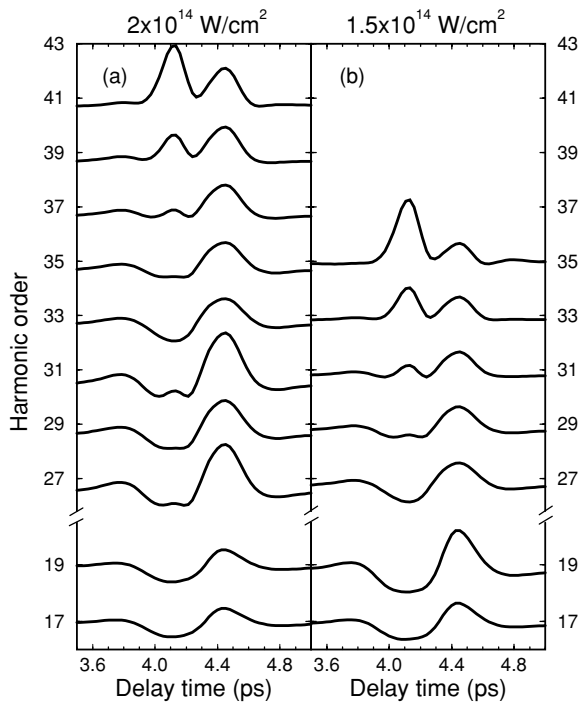


Figure 4. Harmonic signals as functions of delay time near half-revival. The laser intensity is $2 \times 10^{14} \text{ W cm}^{-2}$ (a) and $1.5 \times 10^{14} \text{ W cm}^{-2}$ (b). A (pump) laser pulse of 90 fs duration (FWHM), intensity of $3 \times 10^{13} \text{ W cm}^{-2}$, is used to align the molecules.

contribution dominates at much higher harmonic orders as compared to the lower intensity case shown in the left column. This fact has been noticed earlier by McFarland *et al* [9].

The main results of this paper are presented in figure 4, where we show the harmonic signals as functions of delay time between the pump and probe laser pulses at two intensities of 1.5×10^{14} and $2 \times 10^{14} \text{ W cm}^{-2}$. The signals have been normalized to the signals from the isotropic distribution. These results can be compared directly with the measured HHG signals by McFarland *et al* [9]. Similar to the experiments by McFarland *et al* [9], we take the pump laser polarization to be perpendicular to the probe laser polarization. This is used in order to facilitate the observation of the harmonic signals at the large angles where the HOMO-1 is dominant for high harmonic orders. Theoretically, the harmonic signals are obtained by a coherent convolution of the HHG amplitudes from the QRS calculations with the partial alignment distribution. The time-dependent molecular alignment distribution is calculated by solving the TDSE for N_2 molecules in the pump (alignment) laser field within the rotor model [28]. The pump (alignment) laser has a pulse length of 90 fs (FWHM), intensity of $3 \times 10^{13} \text{ W cm}^{-2}$ and 800 nm wavelength. We assume the Boltzmann distribution for the rotational levels at the initial time and the rotational temperature is taken to be 40 K. The above parameters are chosen to closely match the experimental conditions of McFarland *et al* [9].

At lower laser intensity of $1.5 \times 10^{14} \text{ W cm}^{-2}$, as can be seen from figure 4(b), the lower harmonic (as represented by

H17 and H19) has a minimum at the half-revival near 4.1 ps. In other words, the HHG signal behaves as inverted ($\cos^2 \theta$) (not shown), which measures the degree of molecular alignment. For H29 and higher harmonics, a peak superimposed on the minimum can be seen. This is clear evidence for the increasing importance of the contribution from the HOMO-1 at large angles, shown in figure 3(a). Recall that at the half-revival near 4.1 ps, the molecules are maximally aligned along the pump polarization direction, which is perpendicular to probe polarization. If we artificially remove the HOMO-1 contribution, all the harmonics behave similarly to H17, i.e. as inverted ($\cos^2 \theta$). On the other hand, the contribution from the HOMO-2 is found to be negligibly small and its inclusion does not affect our results. Similar behaviour is seen at higher laser intensity of $2 \times 10^{14} \text{ W cm}^{-2}$ shown in figure 4(a). However, the peak at 4.1 ps starts to show up only at H31 and more systematically after H35. This is due to the fact that the harmonic cutoff is shifted to H35 at this high intensity. It is clear that our QRS theoretical results for a single-molecule response already reproduce quite well the general behaviour reported by McFarland *et al* [9]. We also performed calculations using the standard SFA, with and without including the multiple orbitals, and found that the SFA does not reproduce experimental results. For a more complete theory, one certainly needs to include the macroscopic propagation. As has been reported quite recently by Sickmiller and Jones [29], the phase-matching condition can have a dramatic effect on the HHG signal in the waveguide. The effect of propagation is expected to be much less significant in the gas jet experiment by McFarland *et al* [9] than that in [29]. At present the macroscopic propagation of the HHG in molecular gas media is still largely unexplored with only one attempt for H_2^+ [30] having been reported so far.

In conclusion, by using the recently developed quantitative rescattering theory (QRS) combined with accurate photoionization transition dipoles, we have confirmed theoretically that the peaks superimposed on the minimum near rotational half-revival observed experimentally in N_2 by McFarland *et al* [9] can be attributed to the contribution from the HOMO-1. Our results also show that the contribution from the HOMO-1 becomes more important in the HHG cutoff region and therefore depends on the laser intensity. In this paper, we have limited ourselves to the parallel polarization component for the emitted harmonics, as only the case of orthogonally polarized pump and probe pulses was considered. A recent experiment by Zhou *et al* [31] and an earlier experiment by Levesque *et al* [32], in which the angle between pump and probe polarizations was varied, showed that the ratio of the perpendicular to parallel component intensities could be as high as ~ 0.2 . However, this ratio decreases significantly for large angles between the pump and probe polarizations and goes to zero at 90° due to the symmetry. The importance of this effect is currently under investigation. Finally, we mention the recent experimental and theoretical results by Smirnova *et al* [33], which presented evidence for the multiple orbitals effect in CO_2 .

Acknowledgments

We thank M Gühr, B McFarland, J Farrell and P Bucksbaum for communicating their experimental data to us and for valuable discussions. This work was supported in part by the Chemical Sciences, Geosciences and Biosciences Division, Office of Basic Energy Sciences, Office of Science, US Department of Energy.

References

- [1] Krausz F and Ivanov M 2009 *Rev. Mod. Phys.* **81** 163
- [2] Tong X M, Zhao Z X and Lin C D 2002 *Phys. Rev. A* **66** 033402
- [3] Zhou X X, Tong X M, Zhao Z X and Lin C D 2005 *Phys. Rev. A* **72** 033412
- [4] Madsen C B and Madsen L B 2006 *Phys. Rev. A* **74** 023403
- [5] Itatani J, Zeidler D, Levesque J, Spanner M, Villeneuve D M and Corkum P B 2005 *Phys. Rev. Lett.* **94** 123902
- [6] Kanai T, Minemoto S and Sakai H 2005 *Nature* **435** 470
- [7] Mairesse Y, Levesque J, Dudovich N, Corkum P B and Villeneuve D M 2008 *J. Mod. Optics* **55** 2591
- [8] Thomann I, Lock R, Sharma V, Gagnon E, Pratt S T, Kapteyn H C, Murnane M M and Li W 2008 *J. Phys. Chem. A* **112** 9382
- [9] McFarland B K, Farrell J P, Bucksbaum P H and Gühr M 2008 *Science* **322** 1232
- [10] Le A T, Lucchese R R, Tonzani S, Morishita T and Lin C D 2009 *Phys. Rev. A* **80** 013401
- [11] Stratmann R E and Lucchese R R 1995 *J. Chem. Phys.* **102** 8494
- [12] Lucchese R R, Raseev G and McKoy V 1982 *Phys. Rev. A* **25** 2572
- [13] Le A T, Morishita T and Lin C D 2008 *Phys. Rev. A* **78** 023814
- [14] Morishita T, Le A T, Chen Z and Lin C D 2008 *Phys. Rev. Lett.* **100** 013903
- [15] Le A T, Della Picca R, Fainstein P D, Telnov D A, Lein M and Lin C D 2008 *J. Phys. B: At. Mol. Phys.* **41** 081002
- [16] Le A T, Lucchese R R, Lee M T and Lin C D 2009 *Phys. Rev. Lett.* **102** 203001
- [17] Chen Z, Le A T, Morishita T and Lin C D 2009 *Phys. Rev. A* **79** 033409
- [18] Micheau S, Chen Z, Le A T and Lin C D 2009 *Phys. Rev. A* **79** 013417
- [19] Frolov M V, Manakov N L, Sarantseva T S and Starace A F 2009 *J. Phys. B: At. Mol. Opt. Phys.* **42** 035601
- [20] Frolov M V, Manakov N L and Starace A F 2009 *Phys. Rev. A* **79** 033406
- [21] Cerkick A, Hasovic E, Milosevic D B and Becker W 2009 *Phys. Rev. A* **79** 033413
- [22] Frisch M J *et al* 2003 *GAUSSIAN 03*, revision C.02 (Pittsburgh, PA: Gaussian Inc.)
- [23] Zhao Z X, Tong X M and Lin C D 2003 *Phys. Rev. A* **67** 043404
- [24] Muth-Böhm J, Becker A and Faisal F H 2000 *Phys. Rev. Lett.* **85** 2280
- [25] Litvinyuk I V, Lee K F, Dooley P W, Rayner D M, Villeneuve D M and Corkum P B 2003 *Phys. Rev. Lett.* **90** 233003
- [26] Voss S, Alnaser A S, Tong X M, Maharjan C, Ranitovic P, Ulrich B, Shan B, Chang Z, Lin C D and Cocke C L 2004 *J. Phys. B: At. Mol. Opt. Phys.* **37** 4239
- [27] Telnov D A and Chu S I 2009 *Phys. Rev. A* **79** 041401
- [28] Stapelfeldt H and Seideman T 2003 *Rev. Mod. Phys.* **75** 543
- [29] Sickmiller B A and Jones R R 2009 *Phys. Rev. A* **80** 031802
- [30] Lorin E, Chelkowski S and Bandrauk A 2007 *Comput. Phys. Comm.* **177** 908
- [31] Zhou X, Lock R, Wagner N, Li W, Kapteyn H C and Murnane M M 2009 *Phys. Rev. Lett.* **102** 073902
- [32] Levesque J, Zeidler D, Marangos J P, Corkum P B and Villeneuve D M 2007 *Phys. Rev. Lett.* **98** 183903
- [33] Smirnova O, Mairesse Y, Patchkovskii S, Dudovich N, Villeneuve D, Corkum P and Ivanov M Yu 2009 *Nature* **460** 972